Design and domain structure observation of phase-transition-type negative thermal expansion material

Negative thermal expansion (NTE) materials are expected to be applied in various industrial fields because the thermal expansion can be controlled by mixing an NTE material with a structural material that expands thermally. Among them, recently, materials utilizing large volume changes due to phase transitions have been of particular interest. In phase-transition NTE, the volume change between the low- and high-temperature phases is determined by the parent compound, which results in a trade-off between the transition temperature range and coefficient of thermal expansion. Therefore, the phase transition temperature is adjusted by chemical substitution, which involves selecting a base material with a large volume change. However, this is generally accompanied by a decrease in the volume change [1]. It is of interest to identify types of domains existing inside the particles of a material in which two phases with significantly different volumes coexist and cause NTE due to phase transitions on account of continuous changes in their phase fractions.

This study focuses on the perovskite oxide $PbVO_3$, which exhibits a volume decrease due to the polar–nonpolar phase transition under pressure. Herein, an NTE material is designed with a huge volume change by optimally doping to it, and the coexistence of two phases is observed with a huge volume difference of over 10%. The electron-doped $PbVO_3$ undergoes a polar-to-nonpolar transition accompanied by a very large NTE. The parent compound, $PbVO_3$, has a tetragonal perovskite structure with a space group of *P*4*mm* and large *c*/*a* ratio of 1.23 owing to the ordering of the d_{xy} orbital in addition to the stereo chemical activity of the $6s^2$ lone pair of Pb^{2+} [2,3]. The electron doping reduces the *c*/*a* ratio, whereas the reduction in the $6s^2$ lone pair reduces the transition temperature without reducing the *c*/*a* ratio in $PbVO_3$. In addition, the combination of Bi and Sr substitutions for Pb enables a temperature-induced polar-to-nonpolar transition with a volume shrinkage of 11.1%, which is even larger than the pressure-induced volume collapse of $PbVO_3$ (~10.6%). This value is the largest among those of reported NTE materials (Fig. 1) [4]. The volume difference of the tetragonal and cubic phases in the designed $Pb_{0.8}Bi_{0.1}Sr_{0.1}VO_3$ is as large as 11.1%. An NTE with a volume shrinkage of 9.3% was observed. In addition, in $Pb_{0.775}Bi_{0.125}Sr_{0.1}VO_3$, the temperature hysteresis was reduced after five heating–cooling cycles. This can be attributed to the change in the domain structure. The domain structure of the

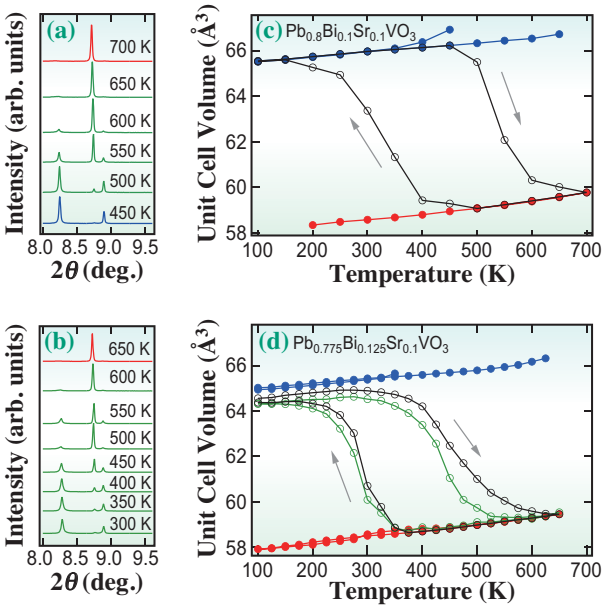

Fig. 1. Temperature variations of synchrotron X-ray diffraction patterns of $Pb_{0.8}Bi_{0.1}Sr_{0.1}VO_3$ **(a)** and $Pb_{0.775}Bi_{0.125}Sr_{0.1}VO_3$ **(b)** around 110_T, 101_T, and 110_C ($\lambda \sim 0.42$ Å). Blue, red, and green denote tetragonal and cubic phases and their coexistence, respectively. Temperature dependences of the unit cell volumes of $Pb_{0.8}Bi_{0.1}Sr_{0.1}VO_3$ **(c)** and $Pb_{0.775}Bi_{0.125}Sr_{0.1}VO_3$ **(d)**. Blue, red, and black denote the tetragonal phase, cubic phase, and weighted average value, respectively. The heating/cooling cycles were repeated for $Pb_{0.775}Bi_{0.125}Sr_{0.1}VO_3$. The first and fifth (green) cycles are plotted.

coexisting cubic and tetragonal phases with a large volume difference of ~10% in $Pb_{0.82}Sr_{0.18}VO_3$ was successfully observed by high-angle annular dark-field scanning transmission electron microscopy (HAADF-STEM).

Figures 2(b) and 2(c) show fast Fourier transform (FFT) images of regions b and c in Fig. 2(a), which indicates that region b has a tetragonal phase with $a = 0.37$ nm and $c = 0.45$ nm, whereas region c has a cubic phase with $a = c = 0.38$ nm. These lattice constants agree well with the results of a Rietveld analysis of the synchrotron X-ray diffraction data. According to the magnified view of the domain boundary shown in Fig. 2(d), the tetragonal and cubic phases are bounded, sharing {110} planes. However, the spacings of the $\{101\}_T$ and $\{110\}_C$ planes exhibit a difference of 10%, which suggests that the mismatch is relaxed by the introduction of a dislocation. The extra half plane of the edge dislocation indicated with the green dashed line exists at every 11 unit cells. The spatial distribution of domains can be evaluated

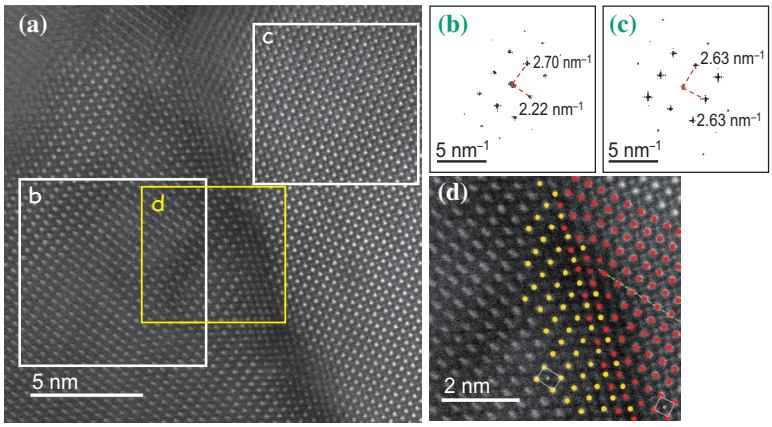

Fig. 2. **(a)** HAADF-STEM image of the cubic–tetragonal boundary in $Pb_{0.82}Sr_{0.18}VO_3$. FFT images of **(b)** tetragonal and **(c)** cubic regions obtained from areas b and c in (a). **(d)** Magnified view of area d in (a) around the phase boundary.

by Bragg coherent X-ray diffraction imaging (BCDI), which is a valuable approach to visualize boundaries of different phases [5]. BCDI was performed at SPring-8 **BL22XU**. The reconstructed three-dimensional image of the particle was obtained by a phase retrieval calculation using a pattern referred to as speckle (Fig. 3(a)). The FFT image of the speckle is shown in Fig. 3(b). The inside isodensity surfaces inside indicate the high cubic 200 reflection density area. Cross-sectional views of the BCDI images are shown in Fig. 3(c). According to the smooth connection of cubic and tetragonal phases, the {110} connection is the most probable, based on the symmetry and elastic energy minimization. In addition, it can be reasonably assumed that the area with a low cubic density sandwiched between areas with high cubic densities is filled with another phase (tetragonal). Figure 3(f) shows a cross-sectional phase image. The phase change indicates the presence of strain at the boundary. The stripes of the phase change are vertical, which is consistent with the vertical boundary of the cubic–tetragonal phases. The overlaying of this image with the dotted line in Fig. 3(e) (the area with a high cubic density) clearly shows the domain boundaries in the phase image in the same area. The phase change is caused by the strain between tetragonal and cubic phases. The temperature hysteresis was reduced by repeated heating/cooling cycles, which suggests that the changes in domain structure dominantly determine the NTE properties. Future studies will focus on clarifying the domain structure change owing to heating–cooling cycles by BCDI.

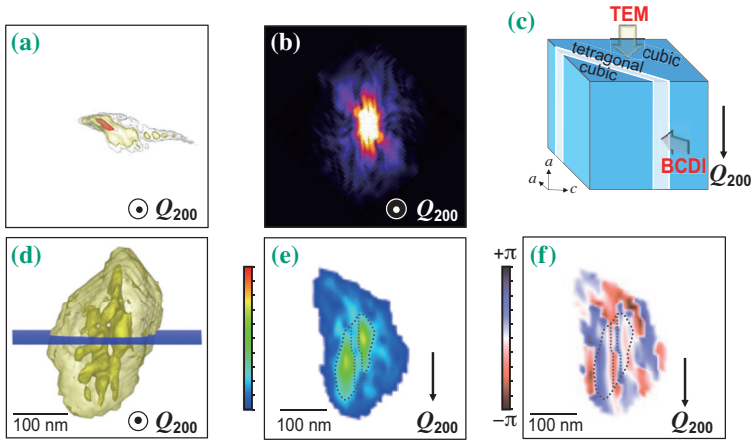

Fig. 3. BCDI of $Pb_{0.82}Sr_{0.18}VO_3$. **(a)** A single recorded diffraction pattern. **(b)** Cross-sectional FFT image of (a). **(c)** Schematic of cubic–tetragonal interfaces. **(d)** Reconstructed three-dimensional image of the particle. **(e)** Cubic 200 reflection density map in the horizontal plane in (c). **(f)** Phase image of the same plane in (e).

Takumi Nishikubo[a,b]

[a] Kanagawa Institute of Industrial Science and Technology
[b] Laboratory for Materials and Structures, Tokyo Institute of Technology

Email: tnishikubo@msl.titech.ac.jp

References

[1] T. Nishikubo *et al.*: J. Am. Chem. Soc. **141** (2019) 19397.
[2] A. A. Belik *et al.*: Chem. Mater. **17** (2005) 269.
[3] H. Yamamoto *et al.*: Angew. Chem. Int. Ed. **57** (2018) 8170.
[4] *T. Nishikubo, T. Imai, Y. Sakai, M. Mizumaki, S. Kawaguchi, N. Oshime, A. Shimada, K. Sugawara, K. Ohwada, A. Machida, T. Watanuki, K. Kurushima, S. Mori, T. Mizokawa and M. Azuma: Chem. Mater.* ***35*** *(2023) 870.*
[5] K. Ohwada *et al.*: Jpn. J. Appl. Phys. **58** (2019) SLLA05.